Turkish Journal of Remote Sensing

https://dergipark.org.tr/en/pub/tuzal

e-ISSN 2687-4997

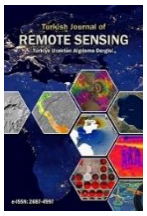

GIS-Based Assessment of Land Surface Temperature Changes Over Khorramabad City (Lorestan, Iran)

Mohammad Hassan Khamesi-Maybodi[*1]

[1]*Yazd University, Technical and Vocational Schools, Yazd, Iran*

Keywords
Land surface temperature
Vegetation
Reflective roof
Remote sensing
Landsat

ABSTRACT

Development of remote sensing applications has led to their use in a wide range of environmental studies. One of these aspects is urban studies and especially land surface temperature. In this study, the changes in land surface temperature in the Khorramabad city in Iran were investigated and the causes of land temperature changes were investigated. For this purpose, Landsat satellite images were processed in four periods of 2000, 2007, 2014 and 2021 and were recovered using a single-channel surface temperature algorithm. Temperatures were high in 2000 due to the type of roofs of buildings and the dirt around the city. Decreased in 2007 and 2014 due to the use of roofs that reflect light. In 2021, due to severe manipulations around the city and the destruction of vegetation and change it into built-up bare soil cover caused the temperature to rise again in the suburbs.

Khorramabad Şehrindeki (Luristan-İran) Arazi Yüzey Sıcaklığı Değişimlerinin CBS Tabanlı Değerlendirilmesi

Anahtar Kelimeler:
Arazi yüzey sıcaklığı
Bitki örtüsü
Yansıtıcı çatı
Uzaktan algılama
Landsat

ÖZ

Uzaktan algılama uygulamalarının gelişmesi, çeşitli çevresel çalışmalarda kullanılmasına yol açmıştır. Bu çalışmalardan biri de kentsel çalışmalar ve özellikle arazi yüzey sıcaklığıdır. Bu çalışmada İran'ın Khorramabad şehrinde arazi yüzey sıcaklığındaki değişimler incelenmiş ve arazi sıcaklık değişimlerinin sebepleri araştırılmıştır. Bu amaçla Landsat uydu görüntüleri 2000, 2007, 2014 ve 2021 olmak üzere dört periyotta işlenmiş ve tek kanallı yüzey sıcaklığı algoritması kullanılarak iyileştirilmiştir. 2000 yılında binalardaki çatı tipi şehrin çevresindeki kirlilik nedeniyle sıcaklıklar yüksekti. 2007 ve 2014 yılları arasında ışığı yansıtan çatıların kullanılması nedeniyle bu sıcaklıklar azalmıştır. 2021 yılında, şehrin etrafındaki şiddetli manipülasyonlar ve bitki örtüsünün yok edilmesi ve çıplak toprak örtüsüne dönüştürülmesi banliyölerde sıcaklığın yeniden yükselmesine neden olmuştur.

* **Corresponding Author**

*(khamesimaybodi@yahoo.com) ORCID ID 0000-0001-8267-3628

Cite this article

Khamesi-Maybodi, M.H. (2022). GIS-based assessment of land surface temperature changes over Khorramabad city (Lorestan, Iran). *Turkish Journal of Remote Sensing*, 4(2) , 87-95.

Research Article / DOI: 10.51489/tuzal.1116553

Received: 13/05/2022; Accepted: 11/11/2022

1. INTRODUCTION

Land surface temperature (LST) is one of the key parameters in the physics of surface processes from local to global scale (Li et al., 2013). The most pressing problem on Earth, especially in urban areas, is rising surface temperatures due to the conversion of vegetation surfaces to impermeable surfaces (Mallick et al., 2008; Pal & Ziaul, 2017). Increasing heat storage capacity at the urban level creates urban heat islands (UHIs) where built-up areas are warmer than adjacent rural areas (Rizwan et al., 2008; Tran et al., 2017). Increasing heat storage capacity at the urban level creates urban heat islands (UHIs) where built-up areas are warmer than adjacent rural areas (Rizwan et al., 2008; Tran et al., 2017).

Global warming is one of the major consequences of human activities in which excessive use of fossil fuels as energy sources increases the concentration of greenhouse gases (GHGs) such as CO2, CH4, N2O and water vapor in the atmosphere, which in itself It itself increases the average surface temperature of the earth (Al-Ghussain, 2019). Direct global warming is difficult to detect because most people experience only local climate change and do not understand long-term global climate trends; Thus, local analysis of climate change may play an important role in adapting behavior and supporting climate change policies (Marx et al., 2007; Spence et al., 2011; Howe et al., 2013). Direct global warming is difficult to detect because most people experience only local climate change and do not understand long-term global climate trends; Thus, local analysis of climate change may play an important role in adapting behavior and supporting climate change policies (Marx et al., 2007; Spence et al., 2011; Howe et al., 2013).

The problem of optimal control for deliberate intervention in the Earth's climate system is considered with the aim of stabilizing the global temperature (Soldatenko & Yusupov, 2019). To date, the goal of measures taken to stabilize global temperature rise (temperature control) below 2° C is probably insufficient (Da Cunha & Eames, 2016). If this goal is to be achieved, more efforts must be made to decarbonize global energy consumption (which still relies heavily on fossil fuel sources) (Hawkes, 2014). Heat island changes depend on many factors, including land use changes (Maleki et al., 2020; Zare Naghadehi et al., 2021), population changes (Manoli et al., 2019), altitude changes (Mathew et al., 2017). Vegetation changes (Gui et al., 2019) and ....

Related research has confirmed that there is an exchange of energy between the Earth's surface and the near-surface atmosphere, and that LST retrieved from thermal infrared remote sensing has a high correlation with air temperature (Shen et al., 2020). Hence, the use of satellite data for LST retrieval is widely used to estimate air temperature (Feizizadeh & Blaschke, 2012; Cammalleri et al., 2012; Hooker et al., 2018; Collados-Lara et al., 2020; Goldblatt et al., 2021). Investigating the city's heat island from the past (Bornstein, 1968; Myrup, 1969; Oke, 1982; Kim, 1992) to the present (Mirzaei, 2015; Yin et al, 2018; He, 2019; Chakraborty, 2020; Halder et al., 2021; Li et al., 2022), has been one of the hottest topics in urban research, especially urban climate. With this introduction, some related research results are presented below.

Hashemi Darebadami et al. (2019) used Modis images to analyze the spatial-temporal of the heat island and its relationship with environmental parameters in Tehran. The results showed that the heat island had daily and seasonal spatial and temporal fluctuations. Maleki et al. (2017) studied the changes of the thermal island of Kermanshah in the period 1393-1397, which showed that the use of reflective roofing has reduced the average temperature. Mansourmoghaddam et al. (1400) in an article on the heat island of Yazd in the period 1990-2020 and concluded that changes in the thermal island boundaries are strongly dependent on land use changes. Hoffmann et al. (2012) examined monthly changes in the city's thermal island; The results showed that the UHI changes were different for different months. The results of Zhang et al. (2013) research showed that changes in land use / land cover and population change led to significant changes in the spatial and temporal patterns of the thermal island due to the loss of water bodies and vegetation levels. A study in the United States found interesting results that indicated the approach of a heat island in urban and rural areas due to changes in rural areas (Scott et al., 2018).

2. STUDY AREA

Khorramabad city is the capital of Lorestan province and the center of Khorramabad city, which is located in the southwest of the country and among the Zagros valleys. This city shares borders with Selseleh city from the north, Andimeshk city from the south, Doroud and Aligudarz cities from the east, and Durah and Poldakhtar cities from the west and southwest. The climate of this city is also temperate and semi-humid Mediterranean (Nikpour et al., 2020). According to the results of the 2016 census, the population of this city was more than 370000 people (Statistics Center of Iran, 2016) and is the 23rd most populous city in Iran (Moradipour et al., 2020). Figure 1 shows a map of the study area.

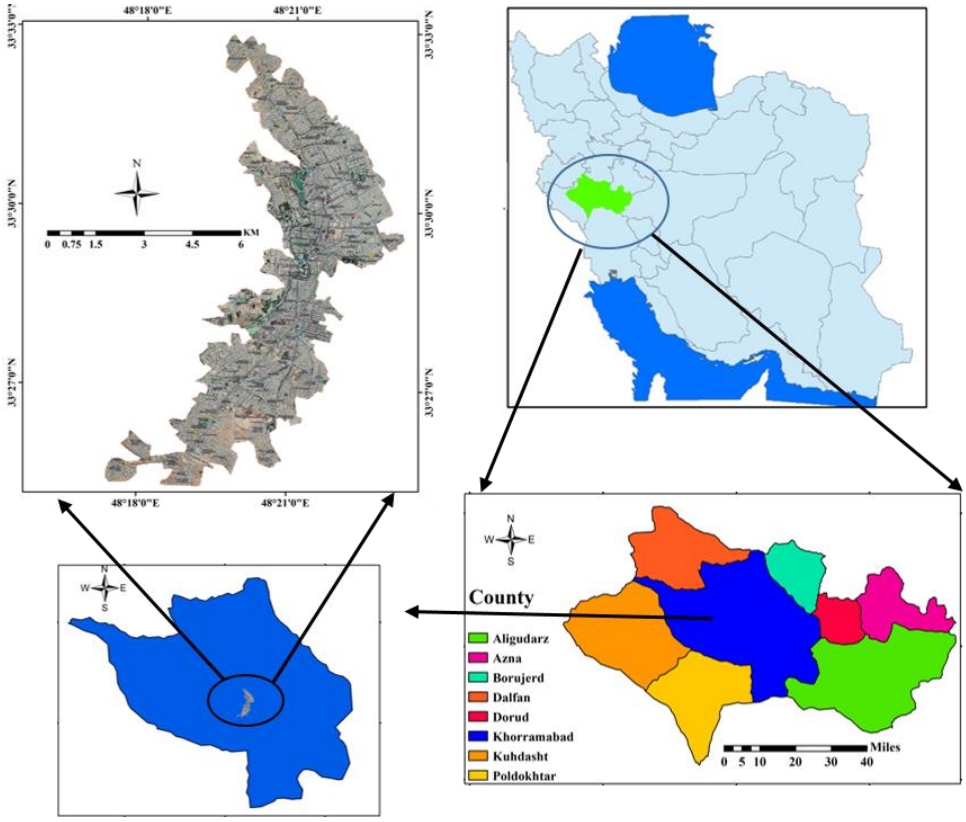

Figure 1. The case study area

3. METODOLOGY

In this study, Landsat satellite images were used to study the temperature changes trend in Khorramabad city. The information about the date and characteristics of the images used in Table 1 is presented. Due to the fact that these images were from two different sensors, the images were register relative to each other to eliminate the effect of geometric distortions. The landsat_gapfill plugin in ENVI software was used to correct the 2007 image Scan Line Corrector (SLC) (Brooks et al., 2018). Also, other preprocessing required to obtain ground surface temperature included spectral radiance (Rajeshwari & Mani, 2014) and reflection coefficient (Sekertekin, 2019).

The amount of income, quality of housing, population aging and youth population. According to past studies, effects of each variable (positive or negative) has been determined. For positive effect we use the symbol of "+" and for negative the symbol of "-". The name of criteria, effectiveness, explanation for each one, extraction method and source for every index is available in Table 1.

Table 1. Images used

S. No	Landsat Name	Landsat Scene ID	Path	Row	Image Acquisition Date
1	ETM+	LE07_L1TP_166037_20000529_20170211	166	37	29/05/2000
2	ETM+	LE07_L1TP_166037_20070618_20170103	166	37	18/06/2007
3	OLI	LC08_L1TP_166037_20140528_20170422	166	37	28/05/2014
4	OLI	LC08_L1TP_166037_20210531_20210608	166	37	31/05/2021

3.1 Brightness Temperature

$$T = \frac{K2}{\ln(\frac{K1}{L_\lambda}+1)} \quad (1)$$

Here T is the brightness temperature of the sensor surface in Kelvin (K), Lλ is high spectral radiation [W / (m ^ 2 sr μm)], K2 is the calibration coefficient in Kelvin, K1 is the calibration coefficient in Kelvin [W / (m ^ 2 sr μm))]. Is The coefficients for Landsat sensors are presented in Table 2.

Table 2. Coefficients K1 and K2 for Landsat sensors

Coefficient / sensor	Landsat 4 and 5TM	Landsat 7 ETM+	Landsat 8 Band 10	Landsat 8 Band 11
K1[W/(m2 Sr μm)]	76/607	09/666	08/1321	1201/14
K2 [kelvin]	56/1260	71/1282	89/777	89/480

3.2 NDVI Vegetation Index

NDVI index plays a large role in energy interactions between the earth and the atmosphere, this index is widely used in the process of retrieving the surface temperature of the earth and can be calculated through Equation 2 (Maleki et al., 2018).

$$NDVI = \frac{\rho_{NIR} - \rho_{RED}}{\rho_{NIR} + \rho_{RED}} \quad (2)$$

In this regard, ρ_NIR is the near-red infinity band reflection and ρ_RED is the red band reflection.

$$\varepsilon = a + b\rho_{red} \quad (FVC = 0)$$
$$\varepsilon = \varepsilon_S(1 - FVC) + \varepsilon_V FVC \quad (0 < FVC < 1)$$
$$\varepsilon = 0.99 \quad (FVC = 1)$$

ρ_red the red band reflectance of the OLI sensor (band 4), a and b are the linear correlation coefficients of the red band reflectance with the surface emissivity, Ɛ_S the radiant power of the soil and Ɛ_V the surface emissivity of the vegetation.

3.5 Land Surface Temperature Retrieval from Single Channel (SC) Algorithm

The SC algorithm used to recover LST from Landsat satellite thermal images was developed by Jiménez-Muñoz et al. (2003) and then (2014). This algorithm applies to all Landsat in the same way with relation 5.

$$T_S = \gamma\left[\frac{1}{\varepsilon}\left(\psi_1 L_{sen} + \psi_2\right) + \psi_3\right] + \delta \quad (5)$$

In this, Ts is the surface temperature, Ɛ is the land surface emissivity of the surface and Lsen is the radiance at the sensor surface. The parameters γ and δ are obtained from Equation 6.

$$\gamma \approx \frac{T_{sen}^{\ 2}}{b_\gamma L_{sen}}; \qquad \delta \approx T_{sen} - \frac{T_{sen}^{\ 2}}{b_\gamma} \quad (6)$$

In this, Tsen is the brightness temperature of the sensor surface, b_γ, which is 1256, 1277 and 1324 for Landsat 5, 7 and 8, respectively (Cristóbal et al., 2018; Sekertekin & Bonafoni, 2020). Ψ_3 〖and Ψ〗 _2 〖, Ψ〗 _ (1) are atmospheric functions that are obtained for Landsat according to Equation 7(Galve et al, 2022).

$$\begin{bmatrix}\psi_1\\ \psi_2\\ \psi_3\end{bmatrix} = \begin{bmatrix}0.04019 & 0.02916 & 1.01523\\ -0.38333 & -1.50294 & 0.20324\\ 0.00918 & 1.36072 & -0.27514\end{bmatrix}\begin{bmatrix}W^2\\ W\\ 1\end{bmatrix} \quad (7)$$

3.3 Vegetation Fraction Cover (FVC)

Fraction Vegetation Cover was estimated from Equation 3. This index can be calculated with the NDVI index and the minimum and maximum values of this index, according to Equation 3.

$$FVC = \left[\frac{NDVI - NDVI_{min}}{NDVI_{max} - NDVI_{min}}\right]^2 \quad (3)$$

Where NDVImin is the lowest NDVI and NDVImax is the highest NDVI (dense vegetation).

3.4 Surface Emissivity

By calculating the vegetation fraction (FVC), the surface emissivity from Equation (4) is calculated.

$$\xrightarrow{TIRS1} = 0.979 - 0.046 r_{OLI-B4}$$
$$\xrightarrow{TIRS2} = 0.982 - 0.027 r_{OLI-B4}$$
$$\xrightarrow{TIRS1} = 0.971(1\text{-FVC}) + 0.987\text{FVC} \quad (4)$$
$$\xrightarrow{TIRS2} = 0.977(1\text{-FVC}) + 0.989\text{FVC}$$

4. RESULTS AND DISCUSSION

After conducting the research stages, the results of land surface temperature in four time periods were determined. Figure 2 shows a map of the land surface temperature in 2000. The map is divided into five classes, the first class of temperatures below 35 degrees and the last class of temperatures above 50 degrees Celsius. According to Figure 2, the urban peripheral had higher temperatures, this is because the area around the city had not yet been built in 2000, and according to studies, bare soil has a higher temperature. This continues almost to the center of the city; Because in these parts, the houses have not been built densely yet. Cool areas on the map are often vegetation.

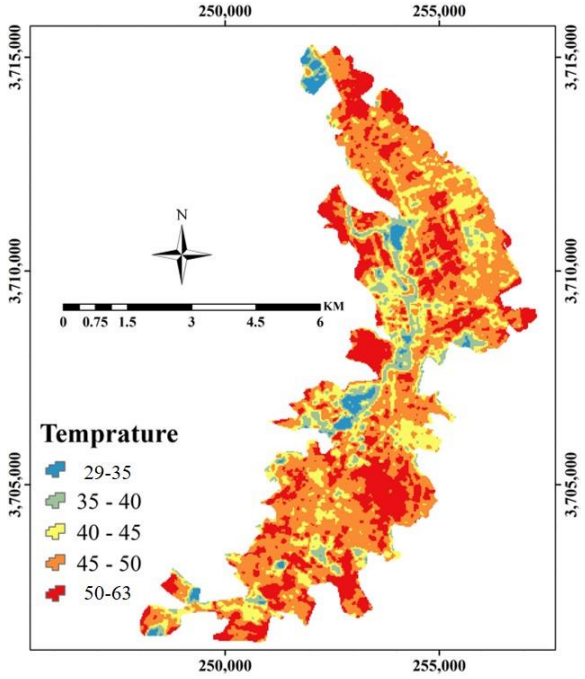

Figure 2. Land surface temperature map of Khorramabad in 2000

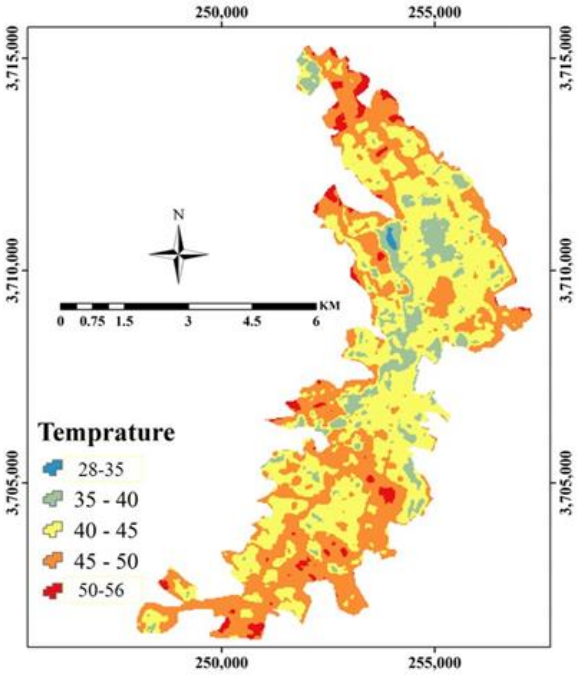

Figure 3. Land surface temperature map of Khorramabad in 2007

According to the information presented in Table 3, the highest area of the city by the fourth class, (the range between 45-50 degrees Celsius), which is about 46% of the city in this area. Then the temperature range is more than 50 degrees, which covers more than 25% of the city.

Table 3. Area of temperature classes of 2000

Class	Area(ha)	Percent
1	942041	2.4%
2	2711531	6.88%
3	7668090	19.47%
4	18110126	45.98%
5	9952428	25.27%

Figure 3 shows the LST map of the city for 2007; According to this figure, it can be seen that the third temperature class (40-45 degrees Celsius) has expanded a lot compared to 2000, but the fourth temperature class still has a wide range.

According to the results presented in the table, the highest temperature range is related to the temperature class of 40-45 degrees with more than 46% of the largest area of the city, but still the temperature range of 45-50 degrees has a large range and more than 40% of the city covered.

Table 4. Area of temperature classes of 2007

Class	Area(ha)	Percent
1	75510	0.19%
2	3906204	9.92%
3	18285953	46.43%
4	15833731	40.2%
5	1282817	3.26%

The land surface temperature map for 2014 shows that the temperatures in the city have progressed towards cooling so that the expansion of the temperature class is 35-40 degrees compared to previous periods, which is quite evident in Figure 4. But the peripheral of the current city area are still the hottest areas because in 2014 the buildings were single and made up mostly of soil.

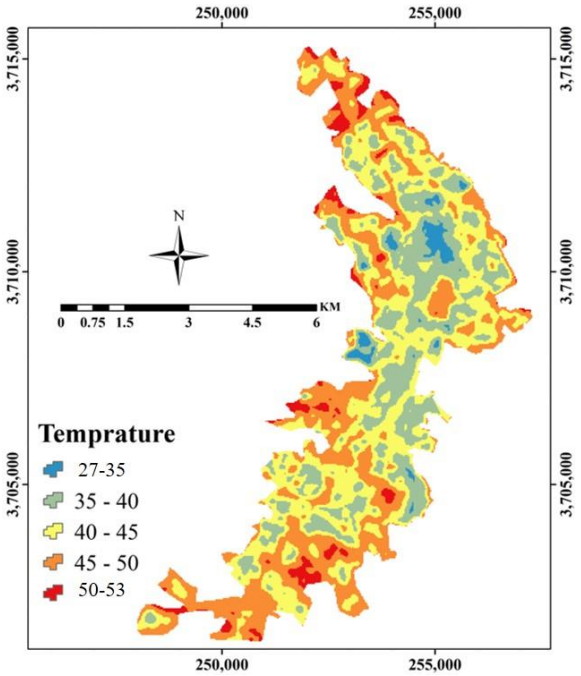

Figure 4. Land surface temperature map of Khorramabad in 2014

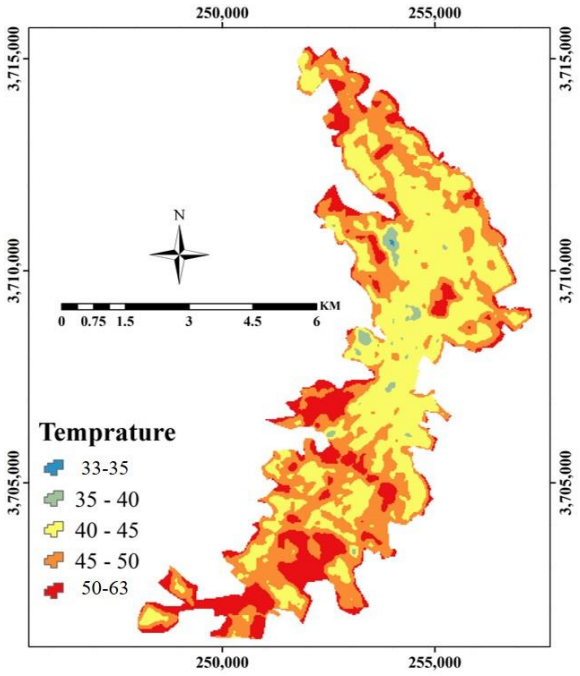

Figure 5. Land surface temperature map of Khorramabad in 2021

Table 5 shows the statistical information of the area and percentage of range covered by each of the temperature classes. According to the information presented in this table, the temperature class has expanded 35-40 degrees and the area of 40-45- and 45-50-degrees classes has been reduced.

Table 5. Area of temperature classes of 2014

Class	Area(ha)	Percent
1	892747	2.11%
2	9221182	23.41%
3	14753712	37.46%
4	12880867	32.71%
5	1698706	4.31%

According to Figure 5, the temperature in the city has risen sharply as temperature classes below 40 ° C are seen in the map as very small areas. But on the other hand, the temperature zones above 40 degrees have increased, which can be said that the greatest increase is related to the temperature class above 50 degrees.

Looking at the statistics presented in Table 6, we will see that the area of the temperature class above 50 degrees has more than quadrupled. On the other hand, the temperature range of less than 40 degrees has been greatly reduced and its temperature zones have been increased to the temperature zones of other classes.

Table 6. Area of temperature classes of 2021

Class	Area(ha)	Percent
1	11833	0.03%
2	473322	1.2%
3	16798862	42.65%
4	15037108	38.18%
5	7063090	17.94%

5. CONCLUSION

Studying how the land surface temperature changes is one of the interesting research topics that many researches are done in the world every year. The thermal island actually shows how cities have higher temperatures than their surroundings. In this study, the land surface temperature changes in the city of Khorramabad in the periods of 2000, 2007, 2014 and 2021 were investigated. The study of the obtained results shows an interesting pattern of temperature changes in the city of Khorramabad. In the first period (2000), a large area of the study area had a temperature range above 50 degrees, which was due to the fact that, firstly, the peripheral sections in 2000 were bare soil zones, which during various studies it has been shown that bare soil often has a higher temperature than the surrounding land uses. Secondly, the roofs of Iranian urban houses in the past (around 2000 and before) were mostly covered with black asphalt and sometimes the roofs of houses were made of dirt. The interesting thing

about the next two periods (2007 and 2014) is that lower temperatures have risen in the city center; This is due to the use of a type of roof covering in recent years, which often has colors that reflect sun radiation (In the past, bitumen and asphalt were used to cover the roof, but in recent years, the use of Waterproofing with colors that reflect sun radiation has reduced LST). Regarding the temperature changes in 2021, the central part of the city is still cooler than the around one's for the reasons mentioned. But the high temperature spread around the city (where in previous times it was not a city, but today it has become a city) this is because the vegetation in these areas has been completely destroyed for construction and replaced by buildings and bare soil (bare soil that are being prepared for construction).

Author contributions

The author declares that has contributed 100% to the article.

Conflicts of Interest

The author declare no conflict of interest.

Declaration of research and publication ethics

In the study, the authors declare that there is no violation of research and publication ethics and that the study does not require ethical committee approval.

REFERENCES

Al-Ghussain, L. (2019). Global warming: review on driving forces and mitigation. *Environmental Progress & Sustainable Energy*, 38(1), 13-21.

Bornstein, R. D. (1968). Observations of the urban heat island effect in New York City. *Journal of Applied Meteorology and Climatology*, 7(4), 575-582.

Brooks, E. B., Wynne, R. H., & Thomas, V. A. (2018). Using window regression to gap-fill Landsat ETM+ post SLC-Off data. *Remote Sensing*, 10(10), 1502.

Cammalleri, C., Anderson, M. C., Ciraolo, G., D'urso, G., Kustas, W. P., La Loggia, G., & Minacapilli, M. (2012). Applications of a remote sensing-based two-source energy balance algorithm for mapping surface fluxes without in situ air temperature observations. *Remote Sensing of Environment*, 124, 502-515.

Chakraborty, T., Hsu, A., Manya, D., & Sheriff, G. (2020). A spatially explicit surface urban heat island database for the United States: Characterization, uncertainties, and possible applications. *ISPRS Journal of Photogrammetry and Remote Sensing*, 168, 74-88.

Collados-Lara, A. J., Fassnacht, S. R., Pardo-Igúzquiza, E., & Pulido-Velazquez, D. (2020). Assessment of high-resolution air temperature fields at rocky mountain national park by combining scarce point measurements with elevation and remote sensing data. *Remote Sensing*, 13(1), 113.

Cristóbal, J., Jiménez-Muñoz, J. C., Prakash, A., Mattar, C., Skoković, D., & Sobrino, J. A. (2018). An improved single-channel method to retrieve land surface temperature from the Landsat-8 thermal band. *Remote Sensing*, 10(3), 431.

Da Cunha, J. P., & Eames, P. (2016). Thermal energy storage for low and medium temperature applications using phase change materials–a review. *Applied energy*, 177, 227-238.

Feizizadeh, B., & Blaschke, T. (2012, July). Thermal remote sensing for land surface temperature monitoring: Maraqeh County, Iran. In 2012 IEEE *International Geoscience and Remote Sensing Symposium* (pp. 2217-2220). IEEE.

Galve, J. M., Sánchez, J. M., García-Santos, V., González-Piqueras, J., Calera, A., & Villodre, J. (2022). Assessment of Land Surface Temperature Estimates from Landsat 8-TIRS in A High-Contrast Semiarid Agroecosystem. Algorithms Intercomparison. *Remote Sensing*, 14(8), 1843.

Goldblatt, R., Addas, A., Crull, D., Maghrabi, A., Levin, G. G., & Rubinyi, S. (2021). Remotely sensed derived land surface temperature (LST) as a proxy for air temperature and thermal comfort at a small geographical scale. *Land*, 10(4), 410.

Gui, X., Wang, L., Yao, R., Yu, D., & Li, C. A. (2019). Investigating the urbanization process and its impact on vegetation change and urban heat island in Wuhan, China. *Environmental Science and Pollution Research*, 26(30), 30808-30825.

Halder, B., Bandyopadhyay, J., & Banik, P. (2021). Monitoring the effect of urban development on urban heat island based on remote sensing and geo-spatial approach in Kolkata and adjacent areas, India. *Sustainable Cities and Society*, 74, 103186.

Hashemi Darebadami, S., Darvishi Boloorani, A., AlaviPanah, S. K., Maleki, Mohammad., & Bayat, R. (2019). Investigation of changes in surface urban heat-island (SUHI) in day and night using multi-temporal MODIS sensor data products (Case Study: Tehran metropolitan). *Journal of*

Applied researches in Geographical Sciences, 19(52), 113-128.

Hawkes, A. D. (2014). Long-run marginal CO2 emissions factors in national electricity systems. *Applied Energy*, 125, 197-205.

He, B. J. (2019). Towards the next generation of green building for urban heat island mitigation: Zero UHI impact building. *Sustainable Cities and Society*, 50, 101647.

Hoffmann, P., Krueger, O., & Schlünzen, K. H. (2012). A statistical model for the urban heat island and its application to a climate change scenario. *International Journal of Climatology*, 32(8), 1238-1248.

Hooker, J., Duveiller, G., & Cescatti, A. (2018). A global dataset of air temperature derived from satellite remote sensing and weather stations. *Scientific data*, 5(1), 1-11.

Howe, P. D., Markowitz, E. M., Lee, T. M., Ko, C. Y., & Leiserowitz, A. (2013). Global perceptions of local temperature change. *Nature climate change*, 3(4), 352-356.

Jiménez-Muñoz, J. C., & Sobrino, J. A. (2003). A generalized single-channel method for retrieving land surface temperature from remote sensing data. *Journal of geophysical research: atmospheres*, 108(D22).

Jiménez-Muñoz, J. C., Sobrino, J. A., Skoković, D., Mattar, C., & Cristóbal, J. (2014). Land surface temperature retrieval methods from Landsat-8 thermal infrared sensor data. *IEEE Geoscience and remote sensing letters*, 11(10), 1840-1843.

Kim, H. H. (1992). Urban heat island. *International Journal of Remote Sensing*, 13(12), 2319-2336.

Li, K., Chen, Y., & Gao, S. (2022). Uncertainty of city-based urban heat island intensity across 1112 global cities: Background reference and cloud coverage. *Remote Sensing of Environment*, 271, 112898.

Li, Z. L., Tang, B. H., Wu, H., Ren, H., Yan, G., Wan, Z., ... & Sobrino, J. A. (2013). Satellite-derived land surface temperature: Current status and perspectives. *Remote sensing of environment*, 131, 14-37.

Maleki, M., Ahmadi, Z., & Dosti, R. (2019). Kermanshah land surface temperature changes in during 1393-1397 periods. *Geography and Human Relationships*, 2(3), 309-319.

Maleki, M., Tavakoli Sabour, S-M & Javan, F. (2018). Analysis of the Effects of Dam Construction on Vegetation of Peripheral Areas in Different Heights and Slopes. Case: Sulayman Shah and Gushan Dam. *Spatial Locational Researches*, 2(2), 102-117.

Maleki, M., Van Genderen, J. L., Tavakkoli-Sabour, S. M., Saleh, S. S., & Babaee, E. (2020). Land use/cover change in dinevar rural area of West Iran during 2000-2018 and its prediction for 2024 and 2030. *Geogr. Tech*, 15, 93-105.

Mallick, J., Kant, Y., & Bharath, B. D. (2008). Estimation of land surface temperature over Delhi using Landsat-7 ETM+. *J. Ind. Geophys. Union*, 12(3), 131-140.

Manoli, G., Fatichi, S., Schläpfer, M., Yu, K., Crowther, T. W., Meili, N., ... & Bou-Zeid, E. (2019). Magnitude of urban heat islands largely explained by climate and population. *Nature*, 573(7772), 55-60.

Mansourmoghaddam, M., Rousta, I., Zamani, M., Mokhtari, M. H., Karimi Firozjaei, M., & Alavipanah, S. K. (2021). Study and prediction of land surface temperature changes of Yazd city: Assessing the proximity and changes of land cover. *Journal of RS and GIS for Natural Resources*, 12(4), 1-27.

Marx, S. M., Weber, E. U., Orlove, B. S., Leiserowitz, A., Krantz, D. H., Roncoli, C., & Phillips, J. (2007). Communication and mental processes: Experiential and analytic processing of uncertain climate information. *Global Environmental Change*, 17(1), 47-58.

Mathew, A., Khandelwal, S., & Kaul, N. (2017). Investigating spatial and seasonal variations of urban heat island effect over Jaipur city and its relationship with vegetation, urbanization and elevation parameters. *Sustainable cities and society*, 35, 157-177.

Mirzaei, P. A. (2015). Recent challenges in modeling of urban heat island. *Sustainable cities and society*, 19, 200-206.

Moradipour, F., Moghimi, E., Beglou, M. J., & Yamani, M. (2020). Assessment of urban geomorphological heritage for urban geotourism development in Khorramabad City, Iran. *Geoheritage*, 12(2), 1-20.

Myrup, L. O. (1969). A numerical model of the urban heat island. *Journal of Applied Meteorology and Climatology*, 8(6), 908-918.

Nikpour, Amer., Soleymani, Mohamad & Mohammadyari, Behnaz (2020) Spatial pattern of factors influencing the formation of poverty zones (Case Study: Khorramabad City). *Urban Economics*, 5(1), 113-126.

Oke, T. R. (1982). The energetic basis of the urban heat island. Quarterly *Journal of the Royal Meteorological Society*, 108(455), 1-24.

Pal, S., & Ziaul, S. K. (2017). Detection of land use and land cover change and land surface temperature in English Bazar urban centre. *The Egyptian Journal of Remote Sensing and Space Science*, 20(1), 125-145.

Rajeshwari, A., & Mani, N. D. (2014). Estimation of land surface temperature of Dindigul district using Landsat 8 data. *International Journal of Research in Engineering and Technology*, 3(5), 122-126.

Rizwan, A. M., Dennis, L. Y., & Chunho, L. I. U. (2008). A review on the generation, determination and mitigation of Urban Heat Island. *Journal of environmental sciences*, 20(1), 120-128.

Scott, A. A., Waugh, D. W., & Zaitchik, B. F. (2018). Reduced Urban Heat Island intensity under warmer conditions. *Environmental Research Letters*, 13(6), 064003.

Sekertekin, A. (2019). Validation of physical radiative transfer equation-based land surface temperature using Landsat 8 satellite imagery and SURFRAD in-situ measurements. *Journal of Atmospheric and Solar-Terrestrial Physics*, 196, 105161.

Sekertekin, A., & Bonafoni, S. (2020). Land surface temperature retrieval from Landsat 5, 7, and 8 over rural areas: Assessment of different retrieval algorithms and emissivity models and toolbox implementation. *Remote Sensing*, 12(2), 294.

Shen, H., Jiang, Y., Li, T., Cheng, Q., Zeng, C., & Zhang, L. (2020). Deep learning-based air temperature mapping by fusing remote sensing, station, simulation and socioeconomic data. *Remote Sensing of Environment*, 240, 111692.

Soldatenko, S. A., & Yusupov, R. M. (2019). Optimal control for the process of using artificial sulfate aerosols for mitigating global warming. *Atmospheric and Oceanic Optics*, 32(1), 55-63.

Spence, A., Poortinga, W., Butler, C., & Pidgeon, N. F. (2011). Perceptions of climate change and willingness to save energy related to flood experience. *Nature climate change*, 1(1), 46-49.

Statistics Center of Iran (2016). Population information.

Syariz, M. A., Jaelani, L. M., Subehi, L., Pamungkas, A., Koenhardono, E. S., & Sulisetyono, A. (2015). Retrieval of sea surface temperature over Poteran Island water of Indonesia with Landsat 8 TIRS image: A preliminary algorithm. *The International Archives of Photogrammetry, Remote Sensing and Spatial Information Sciences*, 40, 87.

Tran, D. X., Pla, F., Latorre-Carmona, P., Myint, S. W., Caetano, M., & Kieu, H. V. (2017). Characterizing the relationship between land use land cover change and land surface temperature. *ISPRS Journal of Photogrammetry and Remote Sensing*, 124, 119-132.

Yin, C., Yuan, M., Lu, Y., Huang, Y., & Liu, Y. (2018). Effects of urban form on the urban heat island effect based on spatial regression model. *Science of the Total Environment*, 634, 696-704.

Zare Naghadehi, S., Asadi, M., Maleki, M., Tavakkoli-Sabour, S. M., Van Genderen, J. L., & Saleh, S. S. (2021). Prediction of Urban Area Expansion with Implementation of MLC, SAM and SVMs' Classifiers Incorporating Artificial Neural Network Using Landsat Data. *ISPRS International Journal of Geo-Information*, 10(8), 513.

Zhang, H., Qi, Z. F., Ye, X. Y., Cai, Y. B., Ma, W. C., & Chen, M. N. (2013). Analysis of land use/land cover change, population shift, and their effects on spatiotemporal patterns of urban heat islands in metropolitan Shanghai, China. *Applied Geography*, 44, 121-133.